Armstrong, E., Valdes, P. J., House, J. I., & Singarayer, J. S. (2016). The Role of CO_2 and Dynamic Vegetation on the Impact of Temperate Land-Use Change in the HadCM3 Coupled Climate Model. *Earth Interactions*, *20*(10). https://doi.org/10.1175/EI-D-15-0036.1

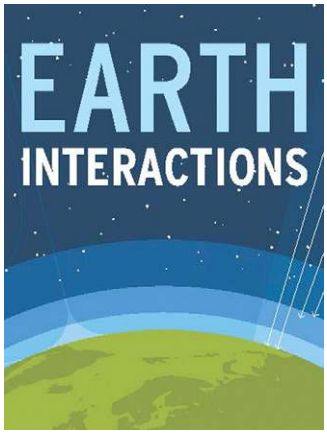

The Role of CO_2 and Dynamic Vegetation on the Impact of Temperate Land-Use Change in the HadCM3 Coupled Climate Model

Edward Armstrong,* Paul Valdes, and Jo House

School of Geographical Sciences, University of Bristol, Bristol, United Kingdom

Joy Singarayer

Centre for Past Climate Change and Department of Meteorology, University of Reading, Reading, United Kingdom

Received 23 June 2015; in final form 9 October 2015

ABSTRACT: Human-induced land-use change (LUC) alters the biogeophysical characteristics of the land surface influencing the surface energy balance. The level of atmospheric CO_2 is expected to increase in the coming century and beyond, modifying temperature and precipitation patterns and altering the distribution and physiology of natural vegetation. It is important to constrain how CO_2-induced climate and vegetation change may influence the regional extent to which LUC alters climate. This sensitivity study uses the HadCM3 coupled climate model under a range of equilibrium forcings to show that the impact of LUC declines under

* Corresponding author address: Edward Armstrong, School of Geographical Sciences, University of Bristol, University Road, Bristol BS8 1SS, United Kingdom.
E-mail address: edward.armstrong@bristol.ac.uk

DOI: 10.1175/EI-D-15-0036.1

increasing atmospheric CO_2, specifically in temperate and boreal regions. A surface energy balance analysis is used to diagnose how these changes occur. In Northern Hemisphere winter this pattern is attributed in part to the decline in winter snow cover and in the summer due to a reduction in latent cooling with higher levels of CO_2. The CO_2-induced change in natural vegetation distribution is also shown to play a significant role. Simulations run at elevated CO_2, yet present-day vegetation show a significantly increased sensitivity to LUC, driven in part by an increase in latent cooling. This study shows that modeling the impact of LUC needs to accurately simulate CO_2-driven changes in precipitation and snowfall and incorporate accurate, dynamic vegetation distribution.

KEYWORDS: Geographic location/entity; Land surface; Physical meteorology and climatology; Albedo; Atmosphere–land interaction; Climate change; Models and modeling; Climate models

1. Introduction

Human-induced land-use change (LUC), such as the conversion of natural land cover to agriculture, transforms the land surface, altering its structure and influencing biogeophysical processes such as albedo, leaf area index (LAI), seasonality, surface roughness, and moisture fluxes. This has implications for the surface energy balance, altering shortwave radiation (SW) and the partitioning of latent and sensible heat (e.g., Brovkin et al. 2009; Bala et al. 2007; Boisier et al. 2012; Pielke et al. 2002). Understanding the climatic impacts of LUC is crucial for improving climate prediction and potential mitigation strategies.

Observed and modeled data show that LUC influences regional and global climate including temperature, precipitation, and humidity (e.g., Bonan 1997; Bonan 2001; Gameda et al. 2007; Ge 2010; Fall et al. 2010; Beltrán-Przekurat et al. 2012; Zhao et al. 2001; Claussen et al. 2001; Bathiany et al. 2010; Chase et al. 2000; Kalnay and Cai 2003; Nuñez et al. 2008; Ezber et al. 2007; Zhao and Jackson 2014; Kumar et al. 2013; Pielke et al. 2007). Studies have shown that the regional response depends on the latitude at which it occurs, which may either enhance or attenuate CO_2-induced warming. Tropical LUC in the form of deforestation acts to warm the climate by suppressing evapotranspiration (Claussen et al. 2001; Snyder et al. 2004; Bathiany et al. 2010), whereas temperate and boreal deforestation is dominated by an increase in albedo and snow persisting longer into the spring, which act to cool the climate (Claussen et al. 2001; Snyder et al. 2004; Bathiany et al. 2010; Davin et al. 2007; Zhao and Jackson 2014; Lee et al. 2011). The opposing temperate and tropical impact of LUC may drive a small global effect; however, its regional-scale impact is likely to be significantly larger (Lawrence and Chase 2010; Brovkin et al. 2013; de Noblet-Ducoudre et al. 2012).

Despite the large number of studies, there remain disparities in modeling results as to the magnitude and sometimes direction of regional and global effects (Pitman et al. 2009; de Noblet-Ducoudre et al. 2012; Brovkin et al. 2013). These inconsistencies have been attributed to differences in how models parameterize albedo, how LUC is implemented, and how crop phenology and evapotranspiration is represented (Pitman et al. 2009).

With levels of atmospheric CO_2 expected to increase in the coming century and beyond, it is important to constrain how the biogeophysical impact of LUC may change under higher CO_2 forcing. A previous study by Pitman et al. (2011) showed that the biogeophysical impact of LUC depended on the background state of the climate. They

attributed a reduction in the winter impact of temperate LUC at higher concentrations of CO_2 to a reduced snow albedo effect. On the contrary, summertime impacts are shown to increase due to CO_2-induced increase in precipitation and latent cooling.

Higher CO_2 concentrations are expected to not only alter the background climate, including temperature and precipitation patterns, but also the distribution and physiology (i.e., stomatal conductance and LAI) of vegetation. We refer to this as land-cover change (LCC), which differs from LUC in that it is a shift from one natural vegetation type to another (e.g., needleleaf to broadleaf vegetation). Increasing CO_2 is expected to drive a northward migration of the tree line and a shift from one dominant vegetation type to another (e.g., O'ishi et al. 2009; Scholze et al. 2006). As with LUC, LCC has implications for the initial biogeophysical characteristics of the land surface including the albedo parameters, roughness length, canopy height, LAI, and rooting depth. This in turn has implications for evapotranspiration and soil moisture availability that can influence climate (e.g., Davies-Barnard et al. 2015; Niyogi and Xue 2006). Stomatal (or canopy) conductance has been shown in laboratory (Field et al. 1995; Brodribb et al. 2009), field (Hungate et al. 2002; Ainsworth and Rogers 2007), and modeling studies (Medlyn et al. 2001; Gopalakrishnan et al. 2011; Collatz et al. 1991; Boucher et al. 2009) to decrease with higher CO_2 concentrations. This effect has been labeled "CO_2 physiological forcing" (Betts et al. 2007a) and acts to decrease evapotranspiration, atmospheric water vapor, and latent cooling and increase surface temperatures (Boucher et al. 2009; Niyogi et al. 2002; Cao et al. 2010).

Many of the current generation of coupled climate models include a land surface component or dynamic global vegetation model (DGVM) that dynamically simulates LCC, including vegetation composition and physiology depending on climate (e.g., Arora 2002). In multimodel studies assessing the biogeophysical impact of LUC, such as Land-Use and Climate, Identification of Robust Impacts (LUCID), only three of the seven modeling groups used dynamic vegetation, and they all used a different initial land-cover distribution (Pitman et al. 2009; Brovkin et al. 2013). This was due to the difficulty in integration and calibration of a common land-cover map. Different vegetation distribution and physiology would be expected to influence the initial conditions of the land surface; however, their relative role in amplifying or attenuating the biogeophysical impact of LUC under higher CO_2 concentrations has not been investigated.

This study will investigate the biogeophysical impact of LUC in the Hadley Centre Coupled Model, version 3 (HadCM3), a coupled climate model with dynamic vegetation [Top-down Representation of Interactive Foliage and Flora Including Dynamics (TRIFFID)] and a land surface scheme [Met Office Surface Exchange Scheme (MOSES); see section 2]. There are two main aims: 1) to examine the impact of LUC under increasing CO_2 concentrations and 2) to assess the importance of dynamic vegetation and LCC simulated by the model and how this influences the extent to which LUC impacts climate. Section 2 gives a description of the HadCM3 climate model and the simulations used in this study. The results are outlined in section 3 followed by an energy balance analysis in section 4. A discussion and summary is presented in section 5.

2. Methods

HadCM3 is a coupled Earth system model comprising a 3D dynamical atmosphere and ocean components and includes a thermodynamic/free-drift sea ice model (Gordon

et al. 2000). The resolution of the atmospheric component is 3.75° × 2.5° with 19 vertical levels, and the ocean resolution is 1.25° × 1.25° with 20 vertical levels.

The model comprises an interactive dynamic vegetation model (TRIFFID; Cox 2001). TRIFFID simulates as a percentage of each grid box with five plant functional types (PFT)—C3/C4 grasses, shrubs, and broadleaf/needleleaf trees—and four nonvegetation types—bare soil, inland water, urban, and ice. Parameters such as albedo and LAI vary for the five PFTs (Table 1), which in turn influence land surface properties such as the surface energy balance. The PFTs vary according to a number of factors including atmospheric CO_2 concentration, temperature, soil carbon availability, and moisture. Soil carbon is calculated by litterfall and microbial respiration, the latter of which is controlled by temperature and soil moisture. Soil carbon and the configuration of PFTs in each grid box are updated every 10 days based on competition from other plants (i.e., trees top the hierarchy before shrubs and grasses) and the fluxes of carbon, which are calculated by the land surface exchange scheme MOSES, version 2.1 (Essery et al. 2003). The updated vegetation distribution is then reentered into MOSES to update land surface parameters such as albedo and surface roughness. This process maintains a consistent hydrological state between the vegetation and atmosphere (Cox 2001). The radiation scheme used in HadCM3 is that of Edwards and Slingo (1996).

MOSES models the physiological processes of transpiration, respiration, and photosynthesis. This links vegetation to CO_2 concentration and atmospheric conditions and impacts the partitioning of surface water. Higher concentrations of CO_2 act to generally decrease canopy conductance that in turn reduces evapotranspiration rate (Boucher et al. 2009). Conductance is also influenced by temperature, soil moisture, and humidity, with the overall effect scaled by LAI. Overall canopy conductance decreases with humidity and increases with soil moisture (Cox et al. 1999), photosynthetically active radiation (PAR) (Sellers et al. 1992), and LAI.

To simulate LUC and conversion to crop and pastureland, natural vegetation was replaced with C3 and C4 grasses (e.g., wheat/rice and sugarcane/maize, respectively) or bare soil using a mask originally derived from Betts et al. (2007b; Figure 1). The mask represents the global disturbed fraction as of the year 1990 constructed with combined pasture values from Goldewijk (2001) and crop fractions from Ramankutty and Foley (1999). The final LUC fraction for the model grid squares is the area designated as per Figure 1, minus that of the three remaining

Table 1. Albedo and LAI values for PFTs simulated by TRIFFID. Albedo values are split into three parameters; sfree is the maximum value for calculating snow-free albedo, and smin and smax are the respective minimum and maximum snow albedos used to calculate the cold deep snow albedo (see Essery et al. 2001). PFT values are based on the International Geosphere–Biosphere Programme (IGBP) classes (Jones 2004).

PFT	Albedo			LAI
	sfree	smin	smax	
Broadleaf	0.10	0.15	0.30	9.0
Needleleaf	0.10	0.15	0.30	6.0
C3 grass	0.20	0.60	0.80	3.0
C4 grass	0.20	0.60	0.80	4.0
Shrub	0.20	0.40	0.80	3.0

nonvegetation types simulated by TRIFFID—that is, inland water, urban, and ice. The model does not include a harvesting or irrigation scheme.

The model was spun up for 1000 years and run at equilibrium for a further 300 years at four CO_2 concentrations: 350, 700, 1050, and 1400 ppm. For each CO_2 concentration, the model was run with and without LUC to isolate its effect. The long spinup period has resulted in the atmosphere reaching an equilibrium state after approximately 1100 years as shown by stabilized global-mean surface air temperatures (SATs; not shown). The LUC mask (Figure 1) is fixed throughout the run, whereas remaining natural vegetation can change. These simulations will hereon be labeled 1×, 2×, 3×, and 4×, respectively, and those with LUC will have the suffix LU. Analysis is performed on the final 50 years of each run, and all anomalies shown are 99% significant as calculated by a Student's *t* test.

To understand the impact of vegetation distribution, a further set of simulations was run at 4× CO_2 but with 1× vegetation distribution (Figure 2a), this is labeled 4×VEG1×. The model was run for 300 years with and without the LUC mask (Figure 1): the former has the suffix LU. The simulations were initialized from the 4× and 4×LU simulations; however, the background vegetation was replaced and initialized with that simulated by the 1× experiment, as shown in Figure 2a. As a result of the initialization, the atmospheric component of the model reaches a relative state of equilibrium after 150 years, as indicated by stabilized global-mean surface air temperatures (not shown). The 4×VEG1× setup represents a simulation with dynamic vegetation switched off and no climatic influence on the distribution of LCC. The 4× CO_2 concentration was used with the 1× vegetation distribution as these represent the extreme end members of our experimental setup. A summary of experiments is shown in Table 2.

3. Results

3.1. Impact of LUC at increasing CO_2 concentrations

Temperature and precipitation anomalies due to the biogeophysical effects of LUC for Northern Hemisphere summer [June–August (JJA)] are shown in Figure 3.

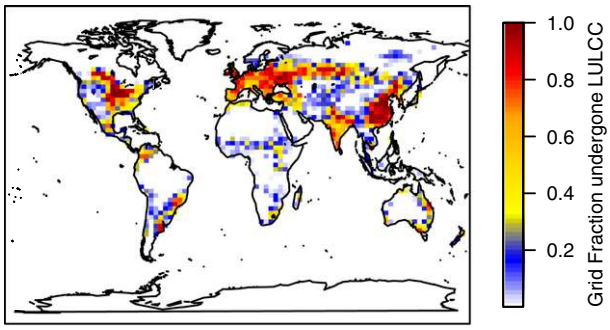

Figure 1. Map showing the proportion of each grid square in HadCM3 that has undergone LUC according to the land-cover mask of **Betts et al. (2007b)**. Final disturbed fraction is calculated with this mask minus the nonvegetation types simulated by TRIFFID.

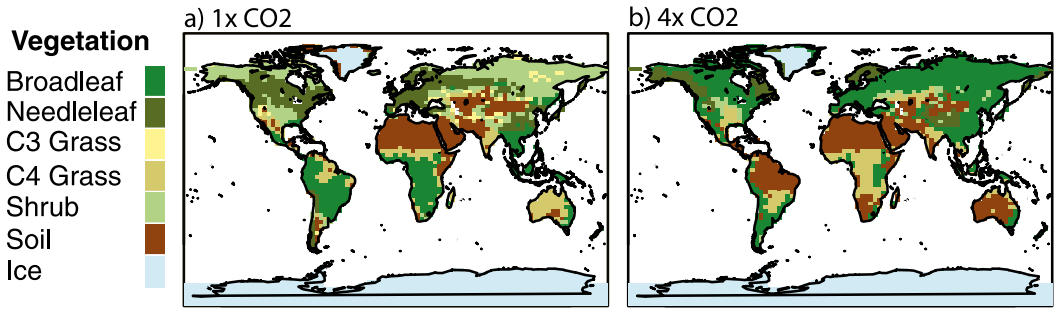

Figure 2. Distribution of natural vegetation simulated by the model occupying greatest proportion of grid square at (a) 1× CO_2 and (b) 4× CO_2.

Mean annual, JJA, and NH winter [December–February (DJF)] anomalies are shown for Europe, North America (NA), and globally for the different model simulations in Figure 4. Table 3 gives the global-mean annual, JJA, and DJF temperature and precipitation values and the anomaly due to LUC in brackets.

LUC acts to cool global SATs for all CO_2 concentrations. The impact at 1× and 2× is comparable but declines globally and regionally for the 3× and 4× simulations. Annual global cooling is in the region of −0.31°C for 1×, decreasing to −0.26°C for 4× (Figures 3, 4). The crop mask has a significantly greater regional and seasonal impact. Cooling is heavily focused in the Northern Hemisphere (NH) midlatitudes peaking at around 50°N (Figure 5), correlating with areas of highest LUC fraction, that is, Europe, NA, and China. Cooling across this midlatitude band peaks in JJA due to higher levels of insolation that drive a greater anomaly in the net absorbed shortwave energy at the surface. European and NA JJA cooling is significantly greater than the global average, decreasing by −1.43° and −1.39°C for 1× and −0.79° and −0.80°C for 4×, respectively.

The overall decrease in SATs due to LUC for all CO_2 concentrations is primarily a response to an increase in surface albedo and reduced SW energy at the surface. Replacement of natural vegetation with C3 and C4 gases increases the maximum canopy/snow albedo parameters in the model (Cox 2001) and reduces LAI. The net surface shortwave energy anomaly peaks in the summer months during periods of highest insolation, whereas the surface albedo anomaly peaks in the winter months due to a significant increase in snow cover. The way in which CO_2 alters the surface energy balance is discussed in section 4.

Table 2. Summary of model simulations. Each simulation was run for 300 years with and without LUC (suffix: LU). Analysis is on the final 50 years of each run; all anomalies are 99% significant as calculated by a Student's *t* test.

Experiment	CO_2 (ppm)	Setup	
1×	350	Equilibrium model run	Each experiment run with and without LUC. Those with LUC have suffix LU.
2×	700	Equilibrium model run	
3×	1050	Equilibrium model run	
4×	1400	Equilibrium model run	
4×VEG	1400	Vegetation fixed at 1× CO_2 distribution	

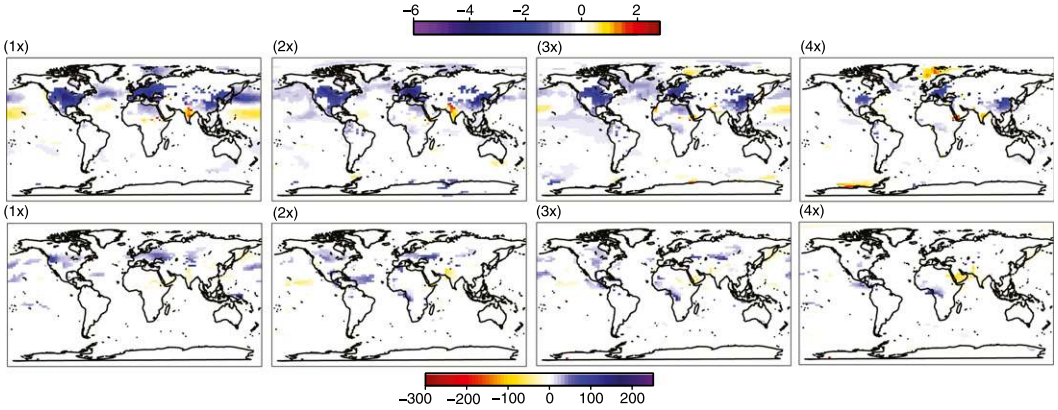

Figure 3. Mean (top) SAT (°C) and (bottom) precipitation (% change) anomalies due to LUC during Northern Hemisphere summer (JJA). Anomalies are 99% confident according to a Student's *t* test.

It is worth noting the contrasting effect seen in India (Figure 3) that experiences a JJA warming peaking at 2.3°C. This pattern was identified in Singarayer et al. (2009) and discussed in more detail by Singarayer and Davies-Barnard (2012), who attributed this to a negative feedback on the monsoon hydrologic cycle. The LUC-driven cooling causes a reduction in convective cloud cover, reducing atmospheric albedo and increasing incoming shortwave (InSW) energy at the surface by up to 3.6 W m^{-2} at 1× $CO_{2\times}$. This acts to counteract the initial cooling impact

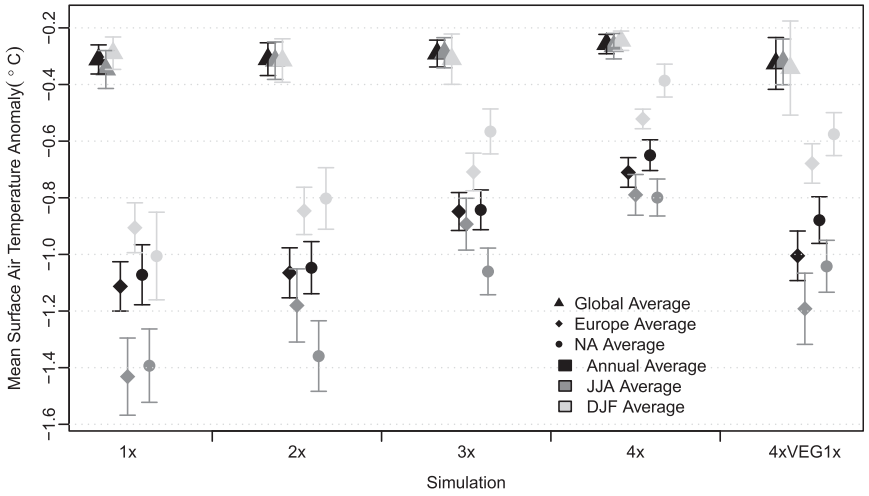

Figure 4. Mean global, European, and NA SAT anomalies due to LUC for the different model simulations (see Table 2 and text for details). Annual, NH, summer (JJA), and NH winter (DJF) are shown. The European region is defined as 35°–60°N and 52.5°E–11.25°W. The North American region is defined as 30°–55°N and 67.5°–123.75°W. Error bars represent the standard error.

Table 3. Mean annual/JJA/DJF SAT and precipitation for experiments. Anomalies due to LUC are shown in brackets.

	SAT (°C)			Precipitation (mm day^{-1})		
Experiment	Annual	JJA	DJF	Annual	JJA	DJF
1×	13.96 (−0.31)	15.63 (−0.27)	12.20 (−0.22)	2.90 (−0.0079)	2.93 (−0.0025)	2.85 (−0.0131)
2×	17.91 (−0.31)	19.69 (−0.25)	16.13 (−0.26)	3.04 (−0.0022)	3.07 (−0.0030)	3.00 (−0.0098)
3×	20.16 (−0.29)	22.00 (−0.23)	18.48 (−0.27)	3.10 (−0.0048)	3.12 (−0.0015)	3.08 (−0.0109)
4×	21.96 (−0.26)	23.85 (−0.21)	20.35 (−0.19)	3.16 (−0.0053)	3.16 (−0.0021)	3.15 (−0.0112)
4× VEG1×	21.20 (−0.33)	23.06 (−0.32)	19.64 (−0.34)	3.08 (−0.0046)	3.09 (−0.0012)	3.08 (−0.0045)

of LUC and also reduces summer precipitation by an average of $-0.42\,\mathrm{mm\,day^{-1}}$ (26%). The potential for LUC to reduce Indian monsoon precipitation has also been shown in the observational study of Niyogi et al. (2010).

LUC influences the surface hydrology and the main flows and partitioning of water. Within HadCM3, precipitation is initially split into canopy interception and throughfall at the surface. Removal of forest and the consequent reduction in LAI decreases canopy interception resulting in a negative annual canopy evaporation anomaly in areas of significant LUC. The increase in throughfall drives a positive anomaly in surface runoff and soil evaporation. Soil moisture anomalies are negative in the top layers, shifting to positive with depth. This reflects the shift from the deep rooting depth associated with forest cover to shallow depths of grasses and therefore greater water extraction in the top layers.

LUC has a small impact on global precipitation, with levels decreasing by $-0.0079\,\mathrm{mm\,day^{-1}}$ for 1× and $-0.0053\,\mathrm{mm\,day^{-1}}$ for 4×. There is a greater regional and seasonal impact, which again is reduced at higher CO_2 concentration. The European precipitation anomaly peaks in the summer (JJA) at $0.16\,\mathrm{mm\,day^{-1}}$ compared to $0.0087\,\mathrm{mm\,day^{-1}}$ change for 4×. The JJA increase in precipitation is most likely a response to the albedo-driven decrease in surface temperature and thus an increase in relative humidity. We would expect that the conversion of natural vegetation to crops would decrease the evapotranspiration rate due to reduced LAI and rooting depth. However, in the HadCM3 climate model, the increase in relative humidity and consequently precipitation counteracts this and drives a net increase in evapotranspiration. There is a reduction in DJF precipitation with LUC in northern temperate and boreal latitudes that may at least in part reflect an increase in snow cover due to reduced SATs and so more water stored on the surface.

The negligible change in precipitation due to LUC at 4× CO_2 is likely in part due to the reduced cooling impact of LUC. However, the influence of CO_2 on canopy conductance is also expected to play a role. Conductance decreases by $-0.0016\,\mathrm{m\,s^{-1}}$ globally with a greater impact over the tropics. This decrease is enhanced in the northern temperate and boreal regions during Northern Hemisphere summer. This is likely to decrease the rate of evapotranspiration and therefore counteract any temperature–humidity-driven increases in precipitation.

3.2. Role of LCC on the impact of LUC

The shift in LCC for 1× and 4× CO_2 is shown in Figure 2. Broadly, there is a northward migration of broadleaf forest, primarily in place of needleleaf vegetation and shrubland. The shift in the tree line is a pattern seen in numerous

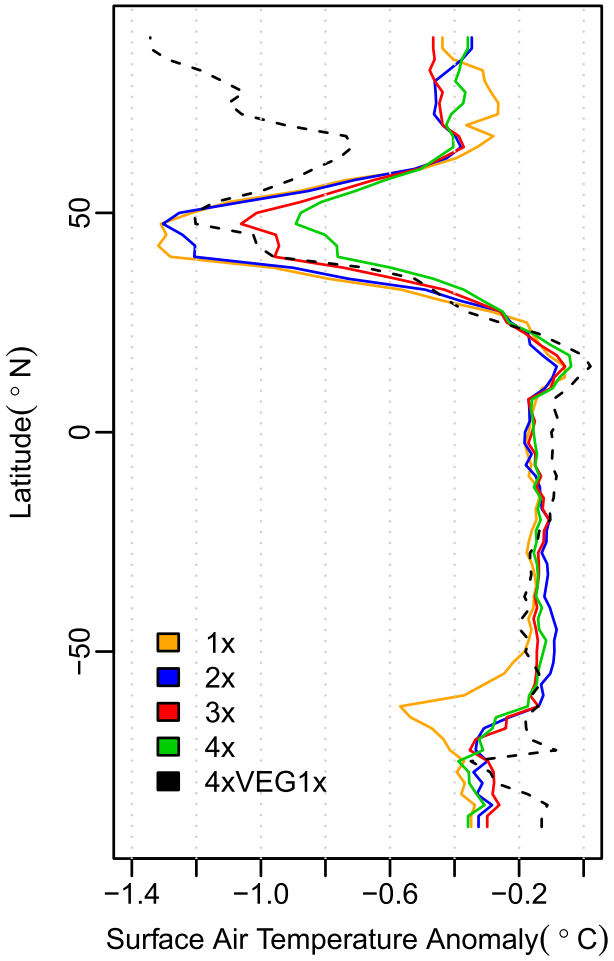

Figure 5. Zonal temperature anomaly during NH summer due to LUC for the five simulations. The dashed black line represents the 4×VEG1× anomaly.

modeling studies (Bala et al. 2006; Lucht et al. 2006; Port et al. 2012; O'ishi et al. 2009; Willeit et al. 2014). There is complete dieback of the Amazon region, a feature apparent in past studies using HadCM3 (Betts et al. 2004; Cox et al. 2000). Other notable impacts include dieback across much of Australia and the decline in the extent of grasses with the exception of sub-Saharan Africa.

The mean temperature and precipitation values for the 4×VEG1× simulation (without LUC) are shown in Table 3. Compared to the 4× simulation, the 4×VEG1× run has lower mean global temperatures on the order of −0.76°C annually. Precipitation levels show a small annual and JJA decline of −0.06 and −0.08 mm day^{-1}, respectively. The cooler global temperatures for 4×Veg1× are primarily driven by higher surface albedo due to the replacement of predominantly broadleaf vegetation with shrubland and needleleaf. There is enhanced cooling impact in the northern boreal regions that may in part reflect an amplification of the positive sea ice albedo feedback. The reduced SATs show that dynamically

simulated vegetation that responds to CO_2 and climate change causes a decrease in surface albedo, acting as a positive feedback on warming.

In Europe and North America, altering vegetation distribution for 4×VEG1× results in a change from predominantly broadleaf vegetation to needleleaf. In Europe, this results in a cooling of −1.34°C; however, the albedo parameters for these forest types are the same in HadCM3. Instead, this cooling may be driven by a reduction in LAI, which is also likely to contribute to a reduction in soil evaporation, transpiration, and consequently precipitation. This also acts to increase soil moisture in the deepest soil level (2 m), the rooting depth of trees.

The annual and seasonal anomalies for the 4×VEG1× simulation are shown in Figure 4, and the zonal impact of LUC for all simulations is shown in Figure 5. The cooling impact of LUC is significantly greater for 4xVEG1x relative to 4×, indicating that natural vegetation distribution simulated by the model has a big effect on the impact of LUC. When background vegetation is allowed to dynamically adjust to CO_2 concentration, the cooling impact of LUC is reduced. The global, JJA, and DJF annual cooling is −0.33°, −0.32°, and −0.34°C, respectively. The more significant winter anomaly is likely to be driven by an increase in high northern latitude sea ice cover, which responds to the greater cooling impact of the crop mask. There is a bigger regional impact, with annual European and North American SAT anomalies of −1.00° and −0.88°C, respectively, peaking at −1.19° and −1.04°C in the summer months.

4. Surface energy balance

To understand the mechanism by which the biogeophysical impact of LUC is altered by CO_2 concentration and the background vegetation distribution, the following analysis focuses on changes in the surface energy fluxes. We concentrate specifically on Europe to provide a more focused analysis; the following results are comparable to the North American region that is not shown here.

Figure 6 shows the JJA and DJF surface energy anomalies due to LUC for the 1×, 4×, and 4×VEG1× simulation. The fluxes of outgoing shortwave (OutSW) are increased due to LUC for all simulations due to an increase in surface albedo. LUC also drives an increase in summer latent energy flux due to increased evapotranspiration, although this effect is small at 4× CO_2. This acts to increase the Bowen ratio (i.e., ratio of latent to sensible heat fluxes) and reduce sensible energy at the surface. The conversion of forest to grassland has been shown in studies to actually decrease latent heat flux (Pitman et al. 2009); however, the increase in precipitation due to the albedo-driven cooling and subsequent increase in relative humidity counteracts this (see section 3.1). The 1× and 4×VEG1× anomalies also show a decrease in incoming SW (not shown) that indicates an increase in atmospheric albedo driven by greater cloud cover due to increased relative humidity, reducing SW reaching the surface and enhancing the cooling impact.

We can compare the JJA and DJF anomalies for the different simulations to indicate how CO_2 concentration and changing LCC influence the impact of LUC. There is a greater cooling effect due to LUC at 1× CO_2 compared to 4× CO_2 in both the summer and winter months; however, they appear to be driven by different factors. In summer, LUC significantly increases latent cooling at 1x CO_2 with only

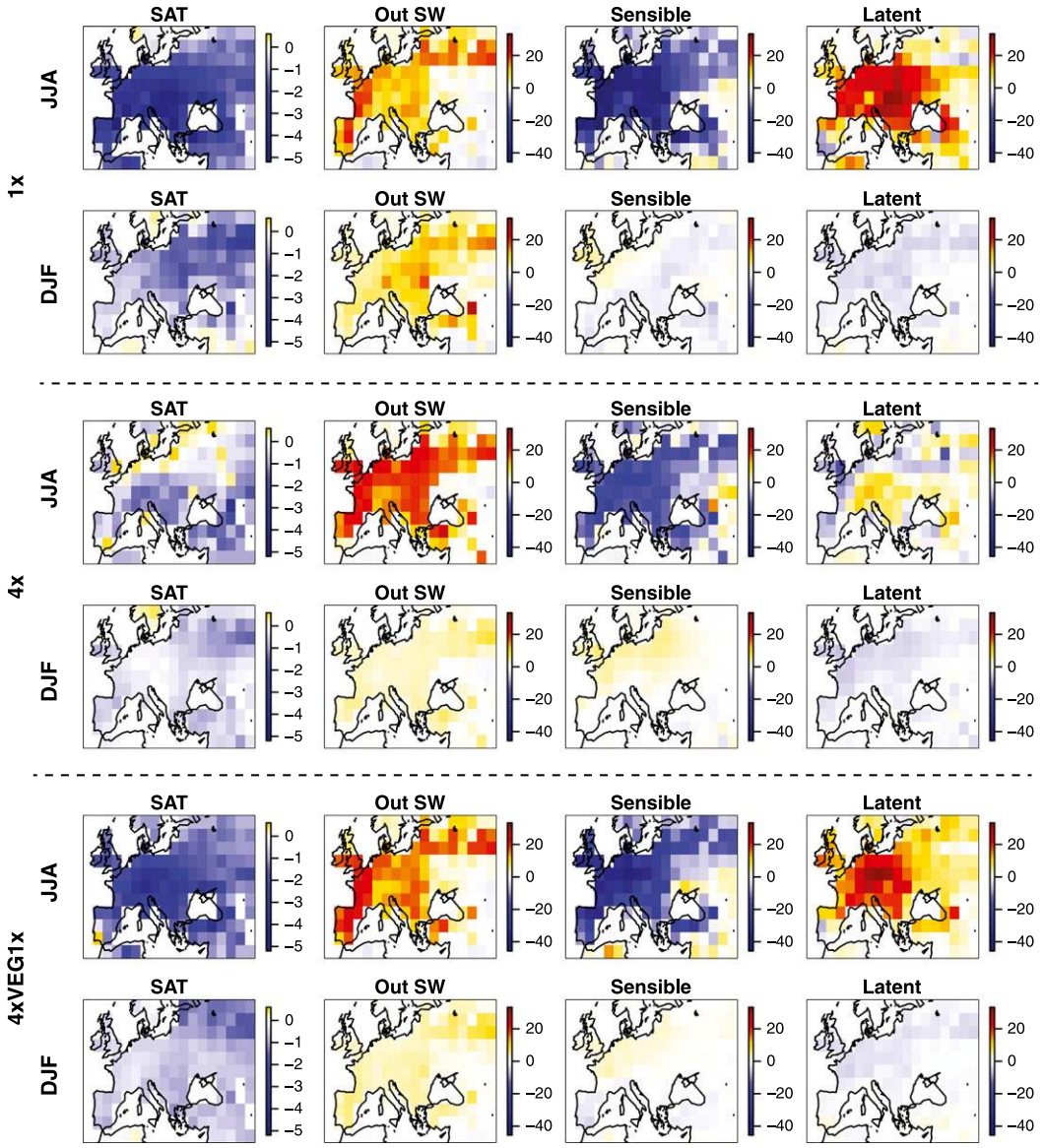

Figure 6. European SAT (°C) and surface energy anomalies (W m^{-2}) due to LUC for Northern Hemisphere summer (JJA) and winter (DJF). (top) 1× CO_2, (middle) 4× CO_2, and (bottom) 4×VEG1× simulation (4× CO_2 but 1× vegetation distribution). OutSW represents outgoing shortwave anomaly. The European region is defined as 35°–60°N and 52.5°E–11.25°W.

a small impact at 4× CO_2. In the winter months, it is not a difference in latent cooling but a greater OutSW anomaly (i.e., albedo) at 1× CO_2 compared to 4× that drives enhanced cooling.

The lesser winter albedo anomaly at 4× CO_2 relative to 1× is likely driven by a weakened snow albedo feedback in a warmer world, an effect highlighted in other

climate modeling studies (e.g., Colman and McAvaney 2009). Figure 7 shows the seasonal cycle for European snow cover for the simulations and the anomaly due to LUC. Mean European DJF snow water equivalent decreases from 21.33 to 2.83 kg m^{-2} for 1× and 4× CO_2 due to warmer temperatures. The impact of LUC is similarly reduced, with European mean DJF snow cover increasing by 1.99 kg m^{-2} for 1×LU and 0.39 kg m^{-2} at 4×LU. This contributes to a smaller increase in winter albedo and indicates a weakened winter cooling effect of LUC under 4× CO_2 concentrations.

In contrast to DJF, the JJA temperature discrepancy is driven not by interactions with snow albedo but with a reduction in latent cooling at higher CO_2. This may in part be driven by CO_2-induced reduction in JJA precipitation over Europe, which declines by 43.2% at 4× CO_2 relative to 1×. This decline may in part be driven by the reduction in canopy conductance due to higher CO_2 concentrations. Consequently, LUC occurs in a more moisture-limited environment at higher CO_2 concentrations. This reduces the rate of evapotranspiration, suppresses latent heat flux, and decreases the JJA cooling impact of LUC. The reduction in precipitation with CO_2 is also expected to decrease cloud cover, increasing InSW at the surface and further counteracting cooling.

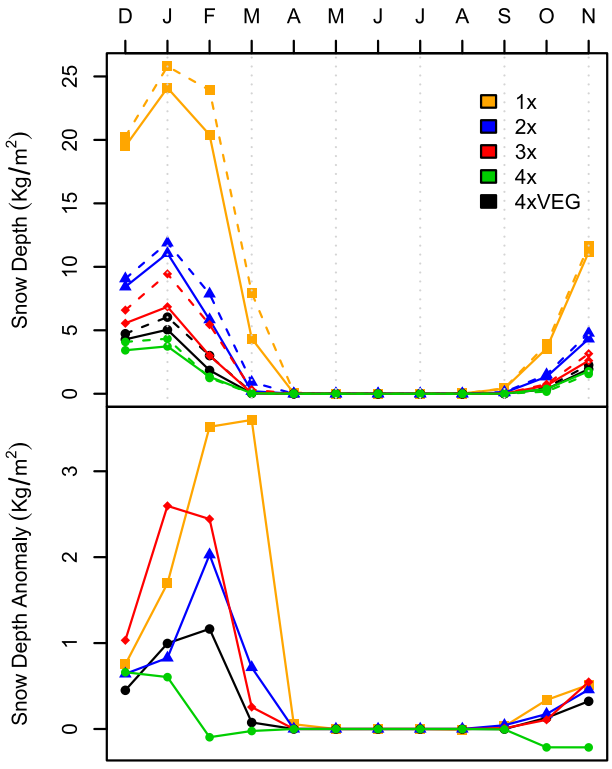

Figure 7. Seasonal cycle of European snow depth (kg m^{-2}) for the four CO_2 concentrations and the 4×VEG1× simulation. Dashed lines in the upper chart are with LUC. The European region is defined as 35°–60°N and 52.5°E–11.25°W.

These results show that CO_2-induced changes in climate, that is, snow cover and precipitation, reduce the impact of LUC in the winter and summer months. To understand the influence of background vegetation, we can compare the 4×VEG1× and 4× anomalies. The JJA cooling impact of LUC is enhanced at 4×VEG1×, driven primarily by an increase in latent cooling. This shows that there is a greater anomaly in latent cooling when LUC is modeled with a 1× CO_2 background vegetation distribution instead of 4×, irrespective of the CO_2 concentration. The enhanced latent cooling is not due to an increase in overall precipitation as it is with 1× and 4× (there is a reduction of 4.3% for 4×VEG1×–4×). Instead, this is likely a response to the way in which water is partitioned at the surface by the vegetation. The 1× vegetation distribution is primarily needleleaf forest that has a lower LAI than broadleaf, influencing canopy height and increasing albedo; consequently, there is a reduction in soil evaporation, transpiration, and latent cooling that produces a positive soil moisture anomaly.

These results show that the decreased JJA impact of LUC under higher CO_2 concentrations is driven not only by the CO_2-induced reduction in overall precipitation but also by the CO_2-induced shift in vegetation and the way in which water is partitioned at the surface. This presents a strong case for the need for models to incorporate dynamic vegetation that is sensitive to climate to accurately simulate the impact of LUC.

It is worth noting that there is a negligible difference in the DJF anomalies between 4×VEG1× and 4×. This is likely due to only a small increase in snow depth and enhancement of the snow albedo effect for 4×VEG1× (Figure 7). This shows that in the winter months, LCC has minimal effect, and it is CO_2-driven changes in snow cover that dominate the overall impact of LUC.

5. Discussion and summary

We have used the HadCM3 coupled climate model to show that LUC cools global climate primarily due to an increase in albedo in temperate regions. The overall global SAT anomaly at a CO_2 concentration of 350 ppm is −0.31°C with a significantly enhanced regional effect in areas of high LUC fraction: Europe, North America, and China. This acts to increase regional precipitation due to an increase in relative humidity. The impact on SAT agrees in sign with a number of previous studies although varies in amplitude (e.g., Brovkin et al. 1999; Govindasamy et al. 2001; Matthews et al. 2004; Betts et al. 2007b).

A simplified flowchart outlining the key processes by which LUC cools climate in HadCM3 is shown in Figure 8a. There are two seasonally dependent positive feedback cycles that act to enhance the cooling impact of LUC. In the winter months, LUC-driven cooling further increases snow cover and surface albedo. In the summer months, cooling increases relative humidity and precipitation, which enhances latent cooling and amplifies cloud albedo.

The first part of this study suggests that the cooling impact of LUC will decrease with higher concentrations of CO_2 due to the breakdown of these positive feedback cycles. The mechanism by which this occurs is shown in Figure 8b. Higher concentrations of CO_2 and warmer conditions decrease winter snow cover (Figure 7) and reduce the degree to which it increases with LUC. The overall effect is to weaken the snow albedo feedback and reduce the cooling impact of LUC in the

winter. In the summer months, an increase in CO_2 is simulated to decrease overall precipitation and consequently reduce the evapotranspiration rate. This reduces the partitioning of latent to sensible energy flux and reduces the cooling effect of LUC. The model also simulates a CO_2-induced decrease in cloud cover, increasing incoming SW energy at the surface and further counteracting cooling. This effect may in part be a response to a reduction in simulated canopy conductance under higher CO_2 concentrations.

These results show that the biogeophysical impact of LUC is dependent on CO_2 concentration and the background climate, an idea initially put forward by Pitman et al. (2011). Their study similarly concluded that the snow albedo mechanism dominates the impact of temperate and boreal LUC in the winter, which is set to diminish with warmer conditions. However, our results presented here disagree with the Pitman et al. (2011) study as to the sign of the summer change under higher CO_2 conditions. They found an increase in summer precipitation under higher CO_2 that drove an increase in latent cooling, the opposite effect to that simulated in HadCM3. Again, this highlights the uncertainty that remains in the modeled response of precipitation to climate change, specifically on a regional scale (see Schaller et al. 2011). However, the general conclusion that the impact of summer LUC is controlled by latent and sensible heat fluxes that are set to change with increasing CO_2 still holds.

The second part of this study investigates the importance of the background vegetation state in quantifying the impact of LUC. Under higher CO_2 concentrations, natural vegetation is expected to change with a general shift of the tree line and conversion of needleleaf and shrubland to broadleaf vegetation. This has implications for the biogeophysical, biogeochemical, and physiological characteristics of the land surface.

Our results show that within the HadCM3 climate model, the regional summer impact of LUC is strongly affected by LCC and the background vegetation type. Again the simplified mechanism for how this occurs is shown in Figure 8b. The shift in natural vegetation with increasing CO_2 alters albedo, LAI, and canopy conductance. These consequently influence the partitioning of water at the surface, reducing soil moisture and transpiration, decreasing latent to sensible energy flux, and counteracting the cooling impact of LUC. When simulating the impact of LUC at $4\times$ CO_2 but with a $1\times$ CO_2 vegetation distribution, cooling is enhanced specifically in the northern temperate regions during summer. This is a response to an increase in latent cooling due to the replacement of predominantly broadleaf vegetation with needleleaf, a reduction in LAI, a suppressed transpiration rate, and higher soil moisture content, enhancing the positive feedback cycles shown in Figure 8a. This shows that the reduced cooling impact of LUC with higher concentrations of CO_2 is driven not only by how the model simulates precipitation patterns, but also how the model dynamically simulates natural vegetation distribution and the way in which this partitions water at the surface.

There remains a high level of uncertainty associated with the impact of LUC in climate models that needs to be addressed in order to assess regional climate change (Pielke et al. 2011). We are aware that there are a number of limitations to our results, namely, that this is a single-model equilibrium experiment using a simplified representation of crops and a relatively simple DGVM. This is

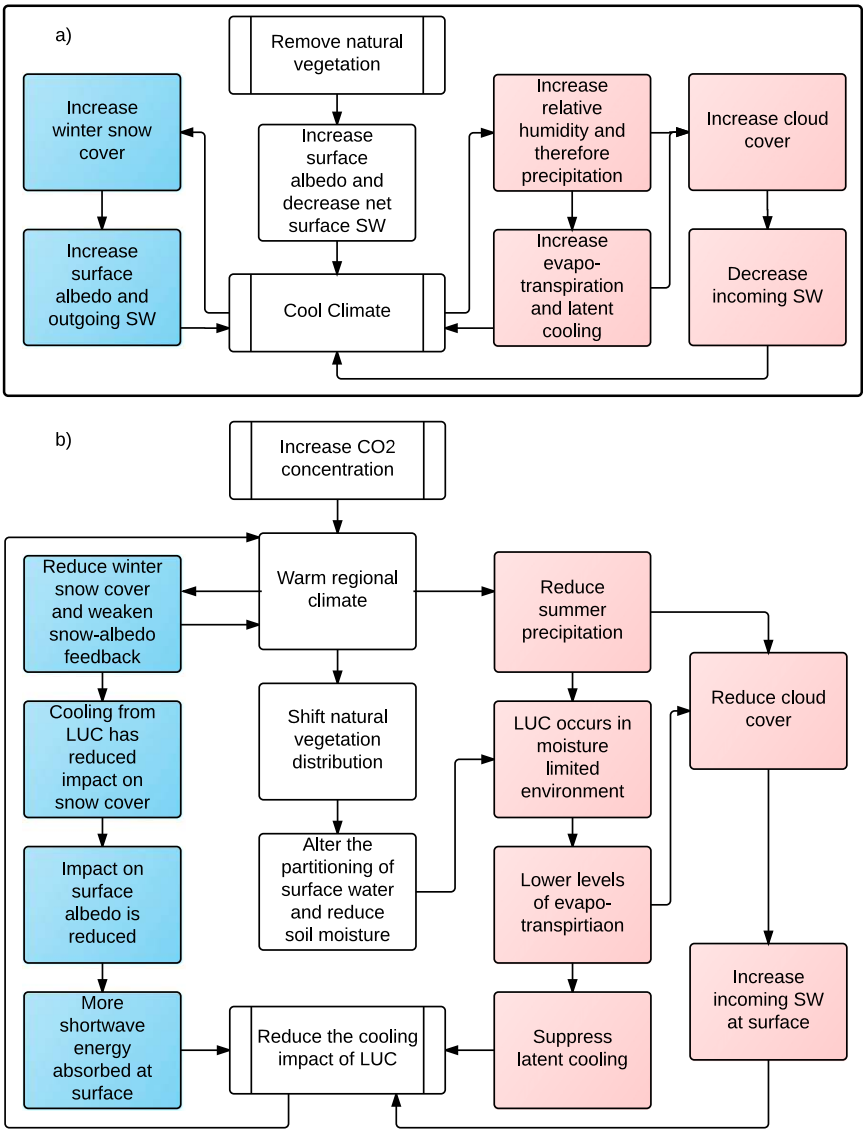

Figure 8. Simplified conceptual flowcharts outlining the key impacts of temperate LUC in HadCM3 and how these are altered by CO_2. (a) The general processes by which LUC causes temperate cooling, and (b) how this cooling impact is reduced under higher concentrations of CO_2 and the role of changing vegetation distribution. The red and blue boxes outline processes that are more prevalent in (although not exclusively) the summer and winter, respectively.

particularly problematic when interpreting the impact and role of precipitation, which remains highly uncertain, yet is crucial to the mechanisms presented in this paper. As a result, the extent and even the sign of changes are likely to be dependent on both the model used and the way in which climate and land-use change have been simulated. As with all modeling studies, a multimodel ensemble would be appropriate in order to validate these mechanisms with a range

of climate models and DGVMs. Also, a perturbed physics ensemble would help determine which specific variable(s) (soil moisture, LAI, albedo, etc.) drive the feedback mechanisms shown in Figure 8b. Building on this, a more comprehensive analysis should also include transient experiments incorporating a range of climate scenarios, such as the representative concentration pathways (RCPs) used in the IPCC report, with different LUC projections. This would not only account for the inconsistencies in models, but also with the uncertainty associated with LUC projections such as the total area and spatial pattern of change. Future projects that may help to address such issues include the Land-Use Model Intercomparison Project (LUMIP), part of the sixth phase of the Coupled Climate Intercomparison Project (CMIP6) with results planned for 2018 to 2019 (see https://cmip.ucar.edu/lumip). This will focus on outstanding uncertainty associated with LUC and may help to elucidate the above mechanisms.

Despite the uncertainty associated with specific mechanisms presented, this study again highlights the potential sensitive of LUC to CO_2 concentration and background climate. This is specifically associated with patterns of precipitation and snowfall and the way in which they may change under higher concentrations of CO_2. As a result, in order to accurately assess the impact of LUC in future projections, modelers need to be aware that the impact of LUC may be influenced by the amount and spatial distribution of these variables at increasing CO_2 concentrations. We also show the potentially important role of background vegetation in quantifying the impact of LUC, a variable that has been largely overlooked in previous studies. As discussed, only three of the seven models used in the LUCID experiment (HadGEM2-ES, MIROC-ESM, and MPI-ESM) incorporated a dynamic vegetation scheme (Pitman et al. 2009; Brovkin et al. 2013). These three models still demonstrate a varied response to LUC due to a range of other inconsistencies, including the way in which land surface processes (i.e., albedo and evapotranspiration) are parameterized and the way LUC is implemented (see Pitman et al. 2009). As such, the direct role of including a dynamic vegetation scheme in these models is not certain. The results of our study indicate that it may potentially be important, and it would be pragmatic to investigate its impact more specifically in future LUC modeling studies.

Acknowledgments. This work was funded by the U.K. National Environmental Research Council (NERC) Grant NE/L501554/1. Our thanks go to the helpful advice of two anonymous reviewers.

References

Ainsworth, E. A., and A. Rogers, 2007: The response of photosynthesis and stomatal conductance to rising [CO_2]: Mechanisms and environmental interactions. *Plant Cell Environ.*, **30**, 258–270, doi:10.1111/j.1365-3040.2007.01641.x.

Arora, V., 2002: Modeling vegetation as a dynamic component in soil-vegetation-atmosphere transfer schemes and hydrological models. *Rev. Geophys.*, **40**, 1006, doi:10.1029/2001RG000103.

Bala, G., K. Caldeira, A. Mirin, M. Wickett, C. Delire, and T. J. Phillips, 2006: Biogeophysical effects of CO_2 fertilization on global climate. *Tellus*, **58B**, 620–627, doi:10.1111/j.1600-0889.2006.00210.x.

——, ——, M. Wickett, T. J. Phillips, D. B. Lobell, C. Delire, and A. Mirin, 2007: Combined climate and carbon-cycle effects of large-scale deforestation. *Proc. Natl. Acad. Sci. USA*, **104**, 6550–6555, doi:10.1073/pnas.0608998104.

Bathiany, S., M. Claussen, V. Brovkin, T. Raddatz, and V. Gayler, 2010: Combined biogeophysical and biogeochemical effects of large-scale forest cover changes in the MPI Earth system model. *Biogeosciences*, **7**, 1383–1399, doi:10.5194/bg-7-1383-2010.

Beltrán-Przekurat, A., R. A. Pielke Sr., J. L. Eastman, and M. B. Coughenour, 2012: Modelling the effects of land-use/land-cover changes on the near-surface atmosphere in southern South America. *Int. J. Climatol.*, **32**, 1206–1225, doi:10.1002/joc.2346.

Betts, R. A., P. M. Cox, M. Collins, P. P. Harris, C. Huntingford, and C. D. Jones, 2004: The role of ecosystem-atmosphere interactions in simulated Amazonian precipitation decrease and forest dieback under global climate warming. *Theor. Appl. Climatol.*, **78**, 157–175, doi:10.1007/s00704-004-0050-y.

——, and Coauthors, 2007a: Projected increase in continental runoff due to plant responses to increasing carbon dioxide. *Nature*, **448**, 1037–1041, doi:10.1038/nature06045.

——, P. D. Falloon, K. K. Goldewijk, and N. Ramankutty, 2007b: Biogeophysical effects of land use on climate: Model simulations of radiative forcing and large-scale temperature change. *Agric. For. Meteor.*, **142**, 216–233, doi:10.1016/j.agrformet.2006.08.021.

Boisier, J. P., and Coauthors, 2012: Attributing the impacts of land-cover changes in temperate regions on surface temperature and heat fluxes to specific causes: Results from the first LUCID set of simulations. *J. Geophys. Res.*, **117**, D12116, doi:10.1029/2011JD017106.

Bonan, G. B., 1997: Effects of land use on the climate of the United States. *Climatic Change*, **37**, 449–486, doi:10.1023/A:1005305708775.

——, 2001: Observational evidence for reduction of daily maximum temperature by croplands in the Midwest United States. *J. Climate*, **14**, 2430–2442, doi:10.1175/1520-0442(2001)014<2430:OEFROD>2.0.CO;2.

Boucher, O., A. Jones, and R. A. Betts, 2009: Climate response to the physiological impact of carbon dioxide on plants in the Met Office Unified Model HadCM3. *Climate Dyn.*, **32**, 237–249, doi:10.1007/s00382-008-0459-6.

Brodribb, T. J., S. A. M. McAdam, G. J. Jordan, and T. S. Feild, 2009: Evolution of stomatal responsiveness to CO_2 and optimization of water-use efficiency among land plants. *New Phytol.*, **183**, 839–847, doi:10.1111/j.1469-8137.2009.02844.x.

Brovkin, V., A. Ganopolski, M. Claussen, C. Kubatzki, and V. Petoukhov, 1999: Modelling climate response to historical land cover change. *Global Ecol. Biogeogr.*, **8**, 509–517, doi:10.1046/j.1365-2699.1999.00169.x.

——, T. Raddatz, C. H. Reick, M. Claussen, and V. Gayler, 2009: Global biogeophysical interactions between forest and climate. *Geophys. Res. Lett.*, **36**, L07405, doi:10.1029/2009GL037543.

——, and Coauthors, 2013: Effect of anthropogenic land-use and land-cover changes on climate and land carbon storage in CMIP5 projections for the twenty-first century. *J. Climate*, **26**, 6859–6881, doi:10.1175/JCLI-D-12-00623.1.

Cao, L., G. Bala, K. Caldeira, R. Nemani, and G. Ban-Weiss, 2010: Importance of carbon dioxide physiological forcing to future climate change. *Proc. Natl. Acad. Sci. USA*, **107**, 9513–9518, doi:10.1073/pnas.0913000107.

Chase, T. N., R. A. Pielke, T. G. F. Kittel, R. R. Nemani, and S. W. Running, 2000: Simulated impacts of historical land cover changes on global climate in northern winter. *Climate Dyn.*, **16**, 93–105, doi:10.1007/s003820050007.

Claussen, M., V. Brovkin, and A. Ganopolski, 2001: Biogeophysical versus biogeochemical feedbacks of large-scale land cover change. *Geophys. Res. Lett.*, **28**, 1011–1014, doi:10.1029/2000GL012471.

Collatz, G. J., J. T. Ball, C. Grivet, and J. A. Berry, 1991: Physiological and environmental regulation of stomatal conductance, photosynthesis and transpiration: A model that includes a laminar boundary layer. *Agric. For. Meteor.*, **54**, 107–136, doi:10.1016/0168-1923(91)90002-8.

Colman, R., and B. McAvaney, 2009: Climate feedbacks under a very broad range of forcing. *Geophys. Res. Lett.*, **36**, L01702, doi:10.1029/2008GL036268.

Cox, P. M., 2001: Description of the "TRIFFID" dynamic global vegetation model. Hadley Centre Tech. Rep. 24, 17 pp. [Available online at http://climate.uvic.ca/model/common/HCTN_24.pdf.]

——, R. A. Betts, C. B. Bunton, R. L. H. Essery, P. R. Rowntree, and J. Smith, 1999: The impact of new land surface physics on the GCM simulation of climate and climate sensitivity. *Climate Dyn.*, **15**, 183–203, doi:10.1007/s003820050276.

——, ——, C. D. Jones, S. A. Spall, and I. J. Totterdell, 2000: Acceleration of global warming due to carbon-cycle feedbacks in a coupled climate model. *Nature*, **408**, 184–187, doi:10.1038/35041539.

Davies-Barnard, T., P. J. Valdes, J. S. Singarayer, A. J. Wiltshire, and C. D. Jones, 2015: Quantifying the relative importance of land cover change from climate and land use in the representative concentration pathways. *Global Biogeochem. Cycles*, **29**, 842–853, doi:10.1002/2014GB004949.

Davin, E. L., N. de Noblet-Ducoudré, and P. Friedlingstein, 2007: Impact of land cover change on surface climate: Relevance of the radiative forcing concept. *Geophys. Res. Lett.*, **34**, L13702, doi:10.1029/2007GL029678.

de Noblet-Ducoudre, N., and Coauthors, 2012: Determining robust impacts of land-use-induced land cover changes on surface climate over North America and Eurasia: Results from the first set of LUCID experiments. *J. Climate*, **25**, 3261–3281, doi:10.1175/JCLI-D-11-00338.1.

Edwards, J. M., and A. Slingo, 1996: Studies with a flexible new radiation code. I: Choosing a configuration for a large-scale model. *Quart. J. Roy. Meteor. Soc.*, **122**, 689–719, doi:10.1002/qj.49712253107.

Essery, R., M. Best, and P. Cox, 2001: MOSES 2.2 technical documentation. Hadley Centre Tech. Note 30, 31 pp. [Available online at http://www.metoffice.gov.uk/media/pdf/9/j/HCTN_30.pdf.]

——, ——, R. A. Betts, P. M. Cox, and C. M. Taylor, 2003: Explicit representation of subgrid heterogeneity in a GCM land surface scheme. *J. Hydrometeor.*, **4**, 530–543, doi:10.1175/1525-7541(2003)004<0530:EROSHI>2.0.CO;2.

Ezber, Y., O. L. Sen, T. Kindap, and M. Karaca, 2007: Climatic effects of urbanization in Istanbul: A statistical and modeling analysis. *Int. J. Climatol.*, **27**, 667–679, doi:10.1002/joc.1420.

Fall, S., D. Niyogi, A. Gluhovsky, R. A. Pielke, E. Kalnay, and G. Rochon, 2010: Impacts of land use land cover on temperature trends over the continental United States: Assessment using the North American Regional Reanalysis. *Int. J. Climatol.*, **30**, 1980–1993, doi:10.1002/joc.1996.

Field, C. B., R. B. Jackson, and H. A. Mooney, 1995: Stomatal responses to increased CO_2: Implications from the plant to the global scale. *Plant Cell Environ.*, **18**, 1214–1225, doi:10.1111/j.1365-3040.1995.tb00630.x.

Gameda, S., B. Qian, C. A. Campbell, and R. L. Desjardins, 2007: Climatic trends associated with summerfallow in the Canadian Prairies. *Agric. For. Meteor.*, **142**, 170–185, doi:10.1016/j.agrformet.2006.03.026.

Ge, J., 2010: MODIS observed impacts of intensive agriculture on surface temperature in the southern Great Plains. *Int. J. Climatol.*, **30**, 1994–2003, doi:10.1002/joc.2093.

Goldewijk, K. K., 2001: Estimating global land use change over the past 300 years: The HYDE database. *Global Biogeochem. Cycles*, **15**, 417–433, doi:10.1029/1999GB001232.

Gopalakrishnan, R., G. Bala, M. Jayaraman, L. Cao, R. Nemani, and N. H. Ravindranath, 2011: Sensitivity of terrestrial water and energy budgets to CO_2-physiological forcing: An investigation using an offline land model. *Environ. Res. Lett.*, **6**, 044013, doi:10.1088/1748-9326/6/4/044013.

Gordon, C., C. Cooper, C. A. Senior, H. Banks, J. M. Gregory, T. C. Johns, J. F. B. Mitchell, and R. A. Wood, 2000: The simulation of SST, sea ice extents and ocean heat transports in a version of the Hadley Centre coupled model without flux adjustments. *Climate Dyn.*, **16**, 147–168, doi:10.1007/s003820050010.

Govindasamy, B., P. B. Duffy, and K. Caldeira, 2001: Land use changes and Northern Hemisphere cooling. *Geophys. Res. Lett.*, **28**, 291–294, doi:10.1029/2000GL006121.

Hungate, B. A., M. Reichstein, P. Dijkstra, D. Johnson, G. Hymus, J. D. Tenhunen, C. R. Hinkle, and B. G. Drake, 2002: Evapotranspiration and soil water content in a scrub-oak woodland under carbon dioxide enrichment. *Global Change Biol.*, **8**, 289–298, doi:10.1046/j.1365-2486.2002.00468.x.

Jones, C. P., 2004: Ancillary file data sources. Unified Model Documentation Paper 70, 42 pp.

Kalnay, E., and M. Cai, 2003: Impact of urbanization and land-use change on climate. *Nature*, **423**, 528–531.

Kumar, S., P. A. Dirmeyer, V. Merwade, T. DelSole, J. M. Adams, and D. Niyogi, 2013: Land use/cover change impacts in CMIP5 climate simulations: A new methodology and 21st century challenges. *J. Geophys. Res. Atmos.*, **118**, 6337–6353, doi:10.1002/jgrd.50463.

Lawrence, P. J., and T. N. Chase, 2010: Investigating the climate impacts of global land cover change in the community climate system model. *Int. J. Climatol.*, **30**, 2066–2087, doi:10.1002/joc.2061.

Lee, X., and Coauthors, 2011: Observed increase in local cooling effect of deforestation at higher latitudes. *Nature*, **479**, 384–387, doi:10.1038/nature10588.

Lucht, W., S. Schaphoff, T. Erbrecht, U. Heyder, and W. Cramer, 2006: Terrestrial vegetation redistribution and carbon balance under climate change. *Carbon Balance Manage.*, **1**, 6, doi:10.1186/1750-0680-1-6.

Matthews, H. D., A. J. Weaver, K. J. Meissner, N. P. Gillett, and M. Eby, 2004: Natural and anthropogenic climate change: Incorporating historical land cover change, vegetation dynamics and the global carbon cycle. *Climate Dyn.*, **22**, 461–479, doi:10.1007/s00382-004-0392-2.

Medlyn, B. E., and Coauthors, 2001: Stomatal conductance of forest species after long-term exposure to elevated CO_2 concentration: A synthesis. *New Phytol.*, **149**, 247–264, doi:10.1046/j.1469-8137.2001.00028.x.

Niyogi, D., and Y. K. Xue, 2006: Soil moisture regulates the biological response of elevated atmospheric CO_2 concentrations in a coupled atmosphere biosphere model. *Global Planet. Change*, **54**, 94–108, doi:10.1016/j.gloplacha.2006.02.016.

——, ——, and S. Raman, 2002: Hydrological land surface response in a tropical regime and a midlatitudinal regime. *J. Hydrometeor.*, **3**, 39–56, doi:10.1175/1525-7541(2002)003<0039:HLSRIA>2.0.CO;2.

——, C. Kishtawal, S. Tripathi, and R. S. Govindaraju, 2010: Observational evidence that agricultural intensification and land use change may be reducing the Indian summer monsoon rainfall. *Water Resour. Res.*, **46**, W03533, doi:10.1029/2008WR007082.

Nuñez, M. N., H. H. Ciapessoni, A. Rolla, E. Kalnay, and M. Cai, 2008: Impact of land use and precipitation changes on surface temperature trends in Argentina. *J. Geophys. Res.*, **113**, D06111, doi:10.1029/2007JD008638.

O'ishi, R., A. Abe-Ouchi, I. C. Prentice, and S. Sitch, 2009: Vegetation dynamics and plant CO_2 responses as positive feedbacks in a greenhouse world. *Geophys. Res. Lett.*, **36**, L11706, doi:10.1029/2009GL038217.

Pielke, R. A., G. Marland, R. A. Betts, T. N. Chase, J. L. Eastman, J. O. Niles, D. D. S. Niyogi, and S. W. Running, 2002: The influence of land-use change and landscape dynamics on the climate system: Relevance to climate-change policy beyond the radiative effect of greenhouse gases. *Philos. Trans. Roy. Soc. London*, **A360**, 1705–1719, doi:10.1098/rsta.2002.1027.

——, J. Adegoke, A. Beltran-Przekurat, C. A. Hiemstra, J. Lin, U. S. Nair, D. Niyogi, and T. E. Nobis, 2007: An overview of regional land-use and land-cover impacts on rainfall. *Tellus*, **59B**, 587–601, doi:10.1111/j.1600-0889.2007.00251.x.

——, and Coauthors, 2011: Land use/land cover changes and climate: Modeling analysis and observational evidence. *Wiley Interdiscip. Rev.: Climate Change*, **2**, 828–850, doi:10.1002/wcc.144.

Pitman, A. J., and Coauthors, 2009: Uncertainties in climate responses to past land cover change: First results from the LUCID intercomparison study. *Geophys. Res. Lett.*, **36**, L14814, doi:10.1029/2009GL039076.

——, F. B. Avila, G. Abramowitz, Y. P. Wang, S. J. Phipps, and N. de Noblet-Ducoudré, 2011: Importance of background climate in determining impact of land-cover change on regional climate. *Nat. Climate Change*, **1**, 472–475, doi:10.1038/nclimate1294.

Port, U., V. Brovkin, and M. Claussen, 2012: The influence of vegetation dynamics on anthropogenic climate change. *Earth Syst. Dyn.*, **3**, 233–243, doi:10.5194/esd-3-233-2012.

Ramankutty, N., and J. A. Foley, 1999: Estimating historical changes in global land cover: Croplands from 1700 to 1992. *Global Biogeochem. Cycles*, **13**, 997–1027, doi:10.1029/1999GB900046.

Schaller, N., I. Mahlstein, J. Cermak, and R. Knutti, 2011: Analyzing precipitation projections: A comparison of different approaches to climate model evaluation. *J. Geophys. Res.*, **116**, D10118, doi:10.1029/2010JD014963.

Scholze, M., W. Knorr, N. W. Arnell, and I. C. Prentice, 2006: A climate-change risk analysis for world ecosystems. *Proc. Natl. Acad. Sci. USA*, **103**, 13 116–13 120, doi:10.1073/pnas.0601816103.

Sellers, P. J., J. A. Berry, G. J. Collatz, C. B. Field, and F. G. Hall, 1992: Canopy reflectance, photosynthesis, and transpiration. III. A reanalysis using improved leaf models and a new canopy integration scheme. *Remote Sens. Environ.*, **42**, 187–216, doi:10.1016/0034-4257(92)90102-P.

Singarayer, J. S., and T. Davies-Barnard, 2012: Regional climate change mitigation with crops: Context and assessment. *Philos. Trans. Roy. Soc. London*, **A370**, 4301–4316, doi:10.1098/rsta.2012.0010.

——, A. Ridgwell, and P. Irvine, 2009: Assessing the benefits of crop albedo bio-geoengineering. *Environ. Res. Lett.*, **4**, 045110, doi:10.1088/1748-9326/4/4/045110.

Snyder, P. K., C. Delire, and J. A. Foley, 2004: Evaluating the influence of different vegetation biomes on the global climate. *Climate Dyn.*, **23**, 279–302, doi:10.1007/s00382-004-0430-0.

Willeit, M., A. Ganopolski, and G. Feulner, 2014: Asymmetry and uncertainties in biogeophysical climate–vegetation feedback over a range of CO_2 forcings. *Biogeosciences*, **11**, 17–32, doi:10.5194/bg-11-17-2014.

Zhao, K. G., and R. B. Jackson, 2014: Biophysical forcings of land-use changes from potential forestry activities in North America. *Ecol. Monogr.*, Vol. 84, Ecological Society of America, 329–353, doi:10.1890/12-1705.1.

Zhao, M., A. J. Pitman, and T. Chase, 2001: The impact of land cover change on the atmospheric circulation. *Climate Dyn.*, **17**, 467–477, doi:10.1007/PL00013740.